



Detection and quantification of trends in time series of significant wave heights: An application in the Mediterranean Sea

Francesco De Leo ^{a,*}, Annalisa De Leo ^a, Giovanni Besio ^a, Riccardo Briganti ^b

^a Department of Civil, Chemical and Environmental Engineering, University of Genoa, Genoa, 16145, Italy

^b Faculty of Engineering, University of Nottingham, Nottingham, NG7 2RD, United Kingdom

ARTICLE INFO

Keywords:

Time series trends
Mann–Kendall test
Theil–Sen slope
Innovative trend analysis
Mediterranean Sea

ABSTRACT

The analysis of long-term trends in time series of wave parameters has an high engineering relevance. These trends may affect the estimates of parameters with high return period that are used for the design of several engineering projects. This work analyses the use of linear regressions for detecting and quantifying long-term trends in time series of data. In particular, the reliability of a linear trend slope, modified in order to minimize the weight of possible outliers, is evaluated. To this end, this slope is compared against the outcomes of two methods that do not imply the hypothesis of linear trend: the Mann–Kendall test and the Innovative Trend Analysis. An application to significant wave height time series over the Mediterranean Sea is presented. Time series of 40 years of numerical hindcast of sea states over the whole basin were analysed, and the methods taken into account were applied to the annual maxima, the annual 98th percentile and the annual mean significant wave height. The results show that the use of the investigated linear slope is meaningful, therefore this was used to assess the spatial distribution of trends in the Mediterranean Sea. Results are presented and discussed for all the statistics investigated.

1. Introduction

Climate change is expected to significantly affect the main met-ocean parameters, at both global and the local scale (Weisse, 2010). Relevant changes are taking place in the upper-sea physics, and in particular in water temperature and salinity (Durack and Wijffels, 2010), large-scale circulation (Cai et al., 2005; Cai and Cowan, 2007), mean sea level (Nicholls and Cazenave, 2010), and wave heights and periods (Vanem, 2016; Morim et al., 2019; Young and Ribal, 2019). In view of these considerations, the evaluation and prediction of the upper-sea physics trends play a crucial role in a plethora of geophysical studies and engineering applications, such as the erosion of the coasts (Stive, 2004), changing design from hard to soft engineering options (Hamm et al., 2002), flooding hazard and coastal vulnerability assessment and management (Adger, 1999; Scavia et al., 2002; Dolan and Walker, 2006; Wdowinski et al., 2016), marine ecosystems (Harley et al., 2006; Richards et al., 2008; Doney et al., 2012). The present study focuses on the variations in wave climate, in particular in trends of significant wave height (henceforth H_s); this is an issue of primary concern, because these may affect the fluxes of energy between the ocean and the atmosphere and even storm surges (Young and Ribal, 2019). These variations would be also important for the coastal areas, as they may in turn modify the equilibrium conditions of coastal beach

profiles (Mori et al., 2010) and affect ports' activity to a substantial extent (Koetse and Rietveld, 2009). It is therefore crucial to identify and quantify the trends in wave climate, to embed these information in engineering design.

The simplest approach to quantify a trend in sea state datasets is to perform a linear regression over the values of the time series. As an instance, Gulev and Grigorieva (2004) applied a linear least square regression to annual mean H_s observed from ship routes over the last century on a global scale. The same approach was used by Shanas and Kumar (2015) to analyse both the annual mean and 90th percentile of H_s in the Central Bay of Bengal, and by Musić and Nicković (2008) in the Eastern Mediterranean, while Appendini et al. (2014) performed linear interpolations of monthly wave height statistics in the Gulf of Mexico. Linear slopes estimates were also employed to characterize extremes H_s selected with the Peak Over Threshold (POT) analysis in the Italian seas (Piscopio et al., 2003), along the Catalan coast (Casas-Prat and Sierra Pedrico, 2010a) and along the Chinese coast (Shi et al., 2019). The hypothesis of linear trend is also adopted in the framework of Non-stationary Extreme Value Analysis (NEVA). Indeed, a pragmatic approach to embed the intra-period trend in the NEVA is that of modelling the distribution parameters as functions of time, and in particular by linearly varying the location parameter in the Generalized Extreme

* Corresponding author.

E-mail address: francesco.deleo@edu.unige.it (F. De Leo).

Value (GEV) and/or the Generalized Pareto distributions (Coles et al., 2001). This approach was applied to several environmental data, such as ocean waves (Méndez et al., 2006; Vanem, 2015; Mentaschi et al., 2016), air temperature (Wang et al., 2013), residual water level and river discharge (Mentaschi et al., 2016), droughts (Burke et al., 2010) etc. However, these methods only allow to evaluate trends in extreme states, since the milder and average ones are not considered in the NEVA.

Previous research made also use of linear regression modified according to the model of Theil–Sen (Sen, 1968; Theil, 1992), resulting in a sounder slope estimate (hereinafter TS slope), because it is insensitive to possible outliers. The TS slope was used, among others, by Pomaro et al. (2017) for the evaluation of monthly quantiles trends in the northern Adriatic Sea, by Young and Ribal (2019) to assess H_s global trends for annual mean, mode and 90th percentile, and by Vanem and Walker (2013), who compared the TS slopes with four different models for detecting long-term trends of H_s in the North Atlantic. In particular, Vanem and Walker (2013) employed the seasonal ARIMA (AutoRegressive Integrated Moving Average) modelling, multiple regression modelling, and GAM (Generalized Additive Model) modelling, and showed that the different approaches result in reasonable agreement. Beside Vanem and Walker (2013), other works performed trend analysis characterized by major complexity than the linear regression over time series of H_s ; among others, Castelle et al. (2018) used a wavelet analysis for assessing the variation in time of the dominant temporal modes of variability in the Atlantic coast of Europe; Muraleedharan et al. (2016) modelled historical trends of extreme H_s in two Portuguese locations through regression quantile models.

In most of the applications that aim to evaluate changes in geophysical time series, the identification of trends is usually carried out using the non-parametric Mann–Kendall statistical test (Mann, 1945; Kendall, 1955, hereinafter called MK), based on the samples rank correlation within a dataset. The MK, as well as many other statistical tests, allows to accept or reject the hypothesis it verifies (the so called *null hypothesis*, in this case the absence of a climate trend) on the basis of the variable p_{value} , defined as the observed significance level for the test hypothesis. The p_{value} is compared to a significance level α , used as a threshold, to reject (if $p_{value} < \alpha$) or accept (if $p_{value} \geq \alpha$) the null hypothesis. In its common use, the MK does not provide any information on the trend magnitude. In the context of trends of H_s , the MK was employed, for example, in the aforementioned studies by Casas-Prat and Sierra Pedrico (2010a) and Pomaro et al. (2017), who selected a threshold of $\alpha = 0.1$ to identify and subsequently characterized locations showing trends off the Catalan coast and in the Adriatic sea, respectively. Similarly, Appendini et al. (2014) and Shi et al. (2019) performed linear interpolations on H_s time series for locations showing trends at a level of α (i.e., threshold level) equal to 0.05.

Nevertheless, it should be mentioned that there is no theoretical basis for the definition of the threshold value α , for that the binary use of p_{value} has been increasingly questioned over the last few years. According to Wasserstein et al. (2016) and Greenland et al. (2016), the p_{value} should be considered as a continuous measure spanning the 0–1 range; 1 indicates that data behave consistently with the null hypothesis, while values tending to zero indicate that data behave progressively less consistently with the null hypothesis. In view of the above, the p_{value} of MK (referred to as p_{MK}) can be used as a measure of compatibility between the data and the hypothesis that they are not characterized by a long-term trend. A similar use of p_{value} is found in Solari et al. (2017), where the p_{value} of the Anderson–Darling statistic was used as a goodness-of-fit measure, to check whether their data were best represented by a Generalized Pareto Distribution. In case of trend analysis, one further limitation of the traditional use of the MK is that a value of α is also required to evaluate the sign of a trend; in fact, the MK statistics has to be evaluated against α to check whether the trend is positive or negative (see Eq. (7) in the present paper). On the contrary,

the slope of the best fitting line immediately reveals whether the data of a series are most likely to increase (positive slopes) or decrease (negative slopes) in time. Indeed, the main advantage of the use of linear slope estimates, is that they provide easy-to-read and prompt information of long-term trends over time series of data, with respect to more complex models which may be difficult to read for many analysts. However, the hypothesis of *linear* rate of change may represent a too limiting assumption.

In this paper, we evaluate whether the TS slope can be efficiently employed to quantify the sign and the magnitude of a trend, even if the underlying trend is not linear. To this end, we take advantage of hindcast data defined over the Mediterranean Sea (MS), computing the annual maxima, the annual mean and the annual 98th percentile of H_s over the whole basin. First, we investigate how the TS slopes of the reference time series relate to their respective p_{MK} ; indeed, MK does not postulate the linearity of the underlying trend. Subsequently, we compare the TS estimates with the outcomes of another method that is not bounded by the hypothesis of linear trend (the so called Innovative Trend Analysis, hereinafter referred to as ITA, Şen, 2011, 2013). Finally, once the suitability of the TS slope for detecting long-term trends is shown, the values of b associated to the hindcast time series are used to evaluate the spatial distribution of long-term trends of the extremes and the mean H_s over the MS.

The paper is structured as follows: in Section 2 we present the hindcast data used for the study, along with the methodologies adopted to detect climate trends throughout the MS and the correlations analysis employed for linking the TS slopes with the methodologies against which they are evaluated. Section 3 shows and discusses the results of the correlation analysis and a regional overview of the trends distributions over the MS. Finally, results are further summarized in Section 4.

2. Data and methods

2.1. Wave hindcast and selection of data

Wave data used here were computed by the hindcast service of the Department of Civil, Chemical and Environmental Engineering of the University of Genoa (Mentaschi et al., 2013, 2015). The service provides the main wave features on a hourly basis over a 40 years long period (from January 1979 to December 2018), with a $0.1273^\circ \times 0.09^\circ$ lon/lat spatial resolution (side of the cells of the computational grid is of the order of 10 km at the latitude of 45°N) over the whole MS. Generation and propagation of sea waves are modelled using WavewatchIII[®] version 3.14 (Tolman, 2009), forced by means of the non-hydrostatic model Weather Research and Forecasting – Advanced Research 3.3.1 (WRF–ARW, Skamarock et al., 2008), based on the Climate Forecast System Reanalysis database (CFSR, Saha et al., 2010). This dataset has been already used for a number of studies on storms and wave climate over the Mediterranean Sea (Besio et al., 2017; De Leo et al., 2019, among others).

In order to detect trends in extreme sea state time series, the events considered to be extremes were extracted from the whole time series of H_s under study. In the extreme value analysis framework, the POT has become a well-established methodology, often preferred to the Annual Maxima (AM) approach, above all for relatively short time series. However, the POT requires to select a H_s threshold that may significantly affect the subsequent trend analysis, either in terms of magnitude and number of resultant peaks (Laface et al., 2016; Liang et al., 2019). The value of the threshold may also be affected by climatic trends, e.g. if the H_s corresponding to the 98th percentile is taken as threshold for the POT, this value will vary in time in presence of a trend. Additionally, the number of events above a given threshold varies every year and different nodes in the grid considered might have different number of events per year, posing additional problems of homogeneity of the reference population, with respect to AM values. On the basis of these considerations, the AM H_s , annual 98th percentile of H_s and annual mean H_s were chosen for the analysis, assuring that one sample per year is used across the grid in all cases.

2.2. Trend detection and quantification

2.2.1. TS method

The simplest trend is a linear one, hence, in order to quantify it, it is possible to use the slope of the linear fit of a series of data. The value of this slope can be computed following the TS method that is insensitive to outliers, and it is therefore preferred to other common tools, such as the least squares regression, for the problem under study (Sen, 1968; Theil, 1992). Considering a series of values x_i ($i = 1 \dots n$, n being the number of samples) the estimate of the TS slope (b) is computed as:

$$b = \text{Median} \left(\frac{x_j - x_l}{j - l} \right) \quad \forall l < j, l, j = 1 \dots n, \quad (1)$$

where x_j and x_l are the j th and l th data of the series, respectively.

2.2.2. The Mann–Kendall test

The MK is aimed at evaluating whether an either upward or downward monotonic trend is present within a dataset (Mann, 1945; Kendall, 1955). The null hypothesis of the test is that there is no monotonic trend in the time series. The test statistic Z_{MK} , considering a time series of n elements x_i , $i = 1 \dots n$, is computed as:

$$Z_{MK} = \frac{\text{num}}{\sqrt{\sigma^2(S)}}, \quad (2)$$

where num is equal to:

$$\text{num} = \begin{cases} S - 1, & \text{if } S > 0 \\ 0, & \text{if } S = 0 \\ S + 1, & \text{if } S < 0, \end{cases} \quad (3)$$

and S and $\sigma^2(S)$ are computed as:

$$S = \sum_{k=1}^{n-1} \sum_{j=k+1}^n \delta_{j-k} \quad (4)$$

$$\sigma^2(S) = \frac{1}{18} \left[n(n-1)(2n+5) - \sum_{p=1}^g t_p(t_p-1)(2t_p+5) \right], \quad (5)$$

with δ_{j-k} being an indicator function that takes 1, 0 or -1 value according to the sign of $x_j - x_k$ (positive, null or negative, respectively); g is the number of tied groups in the time series, with t_p being the number of elements in each p th group ($p = 1, 2, \dots, g$). The value of Z_{MK} is then compared to the percentile of the standard normal distribution, leading to the corresponding p_{MK} of the statistic:

$$p_{MK} = 2\Phi(-|Z_{MK}|), \quad (6)$$

where Φ stands for the cumulative distribution function of the standard normal distribution.

In most of the applications that take advantage of the MK, the p_{MK} is successively compared to α . In such a case, the use of α also allows to detect the sign of the trend (whether it is upward or downward oriented) using the following relationships:

$$\begin{cases} Z_{MK} > \Phi^{-1}(1 - \alpha/2) \rightarrow \text{positive trend} \\ Z_{MK} < -\Phi^{-1}(1 - \alpha/2) \rightarrow \text{negative trend} \\ Z_{MK} < |\Phi^{-1}(1 - \alpha/2)| \rightarrow \text{no trend.} \end{cases} \quad (7)$$

Nevertheless, in this research the p_{MK} of each annual statistic was evaluated in the whole 0–1 range. In this way, p_{MK} was used to assess to what extent the data behave consistently to the hypothesis that they are characterized by the absence of long-term trends.

2.2.3. Innovative trend analysis

The method known as ITA (Şen, 2011, 2013) requires to split a series in two halves, each with elements sorted in ascending order, and plotted versus each other in a square plot. This allows to evaluate how the scatters diverge from the bisecting line, which represents the no-trend condition. Therefore, the ITA allows to quickly check for

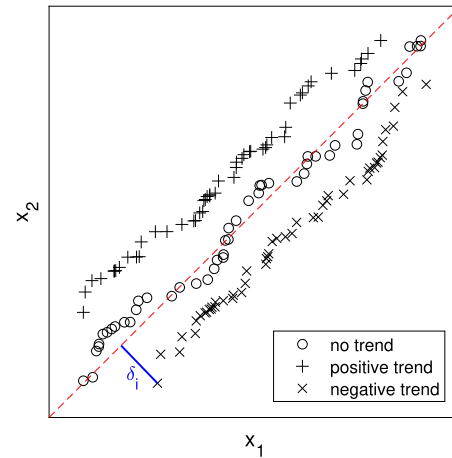


Fig. 1. ITA plot for datasets characterized by positive (black crosses), negative (black x) and no trend (black circles).

increasing or decreasing trends (whether the scatter lies above or below the bisector respectively). An example can be seen in Fig. 1, in which three realizations of generic time series (x_1 and x_2) are first ordered according to the ITA procedure and then plotted against each other; in Fig. 1 δ_i is the distance between the i th ($1 \dots n/2$) element of the series and the no-trend line.

Consequently, for each wave height dataset treated using the ITA, a series of $n/2$ δ_i can be built (where n , in the present analysis, is the number of years over which the hindcast data are defined). Note that the sign of δ_i indicates that the i th value lays below ($\delta_i < 0$) or above ($\delta_i > 0$) the no-trend line. If $\delta_i > 0$ the trend is positive, and it is negative for $\delta_i < 0$, while change in sign of δ_i indicates that not all data behave consistently with the presence of a trend.

2.3. Analysis of the correlation between the variables employed

This study first requires to combine b and p_{MK} without restriction for the rejection of the null hypothesis. Subsequently, b is shown to be correlated with the parameters of the population of δ_i in the ITA method.

2.3.1. Analysis of the rank correlation between b and p_{MK}

The correlation between p_{MK} and b was analysed for all the hindcast locations following Genest and Favre (2007). Correlations were graphically evaluated in the unit-square space, spanning the 0–1 range and populated by the scaled ranks (SR_i) of the investigated variables,

$$SR_i = \frac{m_i}{n+1} \quad (8)$$

where m_i is the position of the i th data within the sorted series it belongs to, whereas n in our case equals the number of years covered by the hindcast. The scatter plot of ranks of p_{MK} versus ranks of b is a visual tool that indicates the presence of correlation, anti-correlation, or no correlation at all. In the case of correlation, high (low) ranks of p_{MK} occur frequently together with high (low) ranks of b . In the case of anti-correlation, high (low) ranks of either variables tend to occur with low (high) ranks of the other. No correlation is characterized by the absence of either of the previous patterns (Genest and Favre, 2007).

Correlation levels were then quantified through the Spearman rank correlation (ρ_s). Said $R_{p,i}$ and $R_{b,i}$ the i th tied ranks of p_{MK} and b respectively, the following expression generally applies:

$$\rho_s = \frac{12}{n(n+1)(n-1)} \sum_{i=1}^n R_{p,i} R_{b,i} - 3 \frac{n+1}{n-1}. \quad (9)$$

Tied ranks are defined as the mean of the ranks of the positions they occupy in the respective sorted dataset. When many ties are

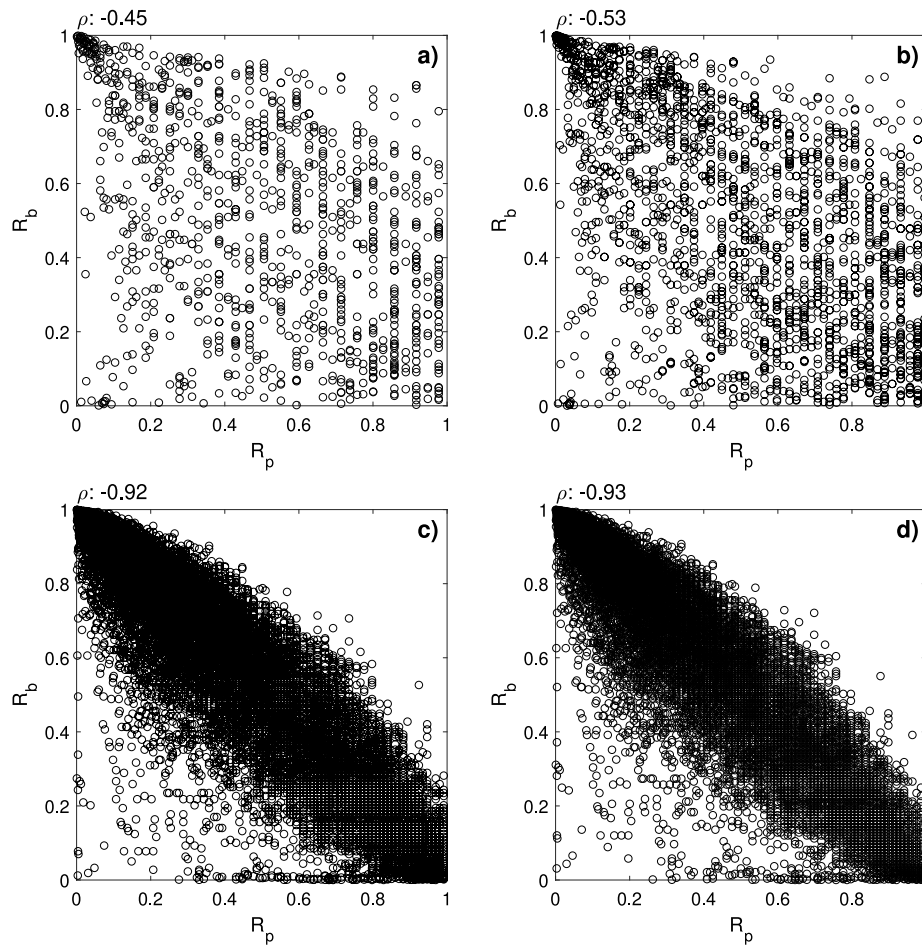


Fig. 2. Correlations between b and p_{MK} due to different values of α . Panel (a): $\alpha = 0.05$; panel (b): $\alpha = 0.1$; panel (c): $\alpha = 0.9$; panel (d): $\alpha = 0.95$.

present in the series to be correlated, a modified formulation of Eq. (9) is available (Zar, 2005). However, in this case the two formulations provided extremely close results, thus only Eq. (9) was used. ρ_s was selected because it has the advantage of being always defined, unlike other commonly employed correlation coefficients, such as the classical Pearson coefficient that directly depends on the second-order moments of the variables of interest, that is not always guaranteed (De Michele et al., 2007). The values of ρ_s span from -1 (for series perfectly anti-correlated) to 1 (series perfectly correlated); ρ_s equal to 0 indicates that no correlation exists between the investigated series. Correlations were iteratively evaluated by varying the significance level α within the $0-1$ range with a 0.01 incremental step. For every iteration, only the series with $p_{MK} < \alpha$ were retained for the analysis, i.e. just the series allowing to reject the MK null hypothesis according to the binary use of p_{MK} . When α equals 1 , no data are excluded and all the hindcast locations are taken into account; indeed, the maximum value that p_{MK} can attain is exactly 1 , therefore in the latter case no filtering of the series due to the value of α is applied.

2.3.2. Analysis of the correlation between b and the distribution of δ_i

The second step of the developed study, requires to check whether the values of b are consistent with the δ_i obtained by the ITA, with reference to the respective series (i.e. the H_s annual statistics of the hindcast locations).

The reliability of the linear trend hypothesis was first evaluated by analysing the empirical cumulative distribution function (ecdf) of δ_i series for four hindcast locations characterized by different values of b . This allows to check rapidly if the δ_i series increase or decrease

according to the values of b the ecdf is linked to, meaning that the larger is b , the larger are the δ_i .

However, a graphical comparison for all the hindcast locations was not feasible due to the high number of available datasets. Therefore, the sum of the δ_i for each H_s time series was computed using this sum as a single parameter for the analysis instead of $n/2$ data. This allowed to perform a direct comparison between datasets of equal length (e.g. the number of hindcast locations): one containing the values of b and the other with the sum of δ_i (for each of the annual statistics taken into account).

3. Results

3.1. Trend analysis: comparison of the different methods

First, the scatter plots between b and p_{MK} for the AM H_s are shown in Fig. 2, indicating their correlation. For the sake of clarity, only results for four levels of α are here reported (0.01 , 0.05 , 0.90 , and 0.95). The panels show as well the values of ρ_s computed for the AM H_s series showing $p_{MK} \leq \alpha$.

The series with $p_{MK} < \alpha$, $\alpha = 0.05|0.1$ (Fig. 2, panels (a) and (b)), show moderate correlation between p_{MK} and b . In fact, the scatters of R_b and R_p are almost randomly distributed over the square-unit space, and the values of the respective ρ_s are far from -1 , which would indicate a perfect anti-correlation. On the other hand, analysing the correlation for p_{MK} retained considering higher values of α ($0.9|0.95$, Fig. 2 panels (c) and (d)), shows a very strong anti-correlation between the two investigated parameters. As shown by the distributions of R_p and R_b in panels (c) and (d) of Fig. 2, low values of p_{MK} are most

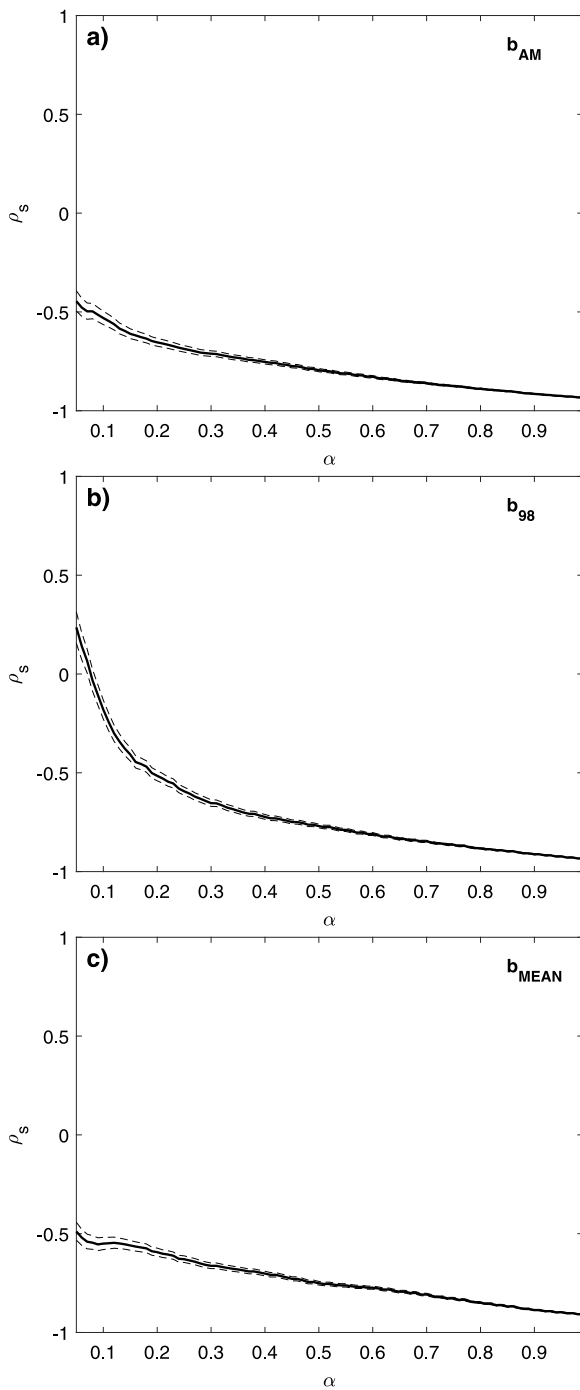


Fig. 3. ρ_s for the correlation between b and p_{MK} for different values of α . Panel (a): AM data; panel (b): annual 98th percentile of H_s ; panel (c): annual mean H_s . Confidence bounds were computed according to Bonett and Wright (2000) (dashed curves).

likely to occur when b attains high values and vice-versa: the scaled ranks are less scattered around the -1 bisector (even though a lack of symmetry between the lower left and the upper right corners can be still appreciated), and ρ_s reaches values close to -1 . As explained in Section 2.3.1, the full range of α was explored; Fig. 3 shows the results of ρ_s as a function of α . For the sake of clarity, hereinafter values of b related to the AM, annual 98th percentile and annual mean H_s are referred to as b_{AM} , b_{98} and b_{MEAN} , respectively. In panel (a) of Fig. 3 it can be noticed how the anti-correlation between p_{MK} and b_{AM} becomes stronger (i.e. ρ_s tends to -1) proportionally to the level of α taken into account. Similar outcomes were found for b_{98} and b_{MEAN} ; in these

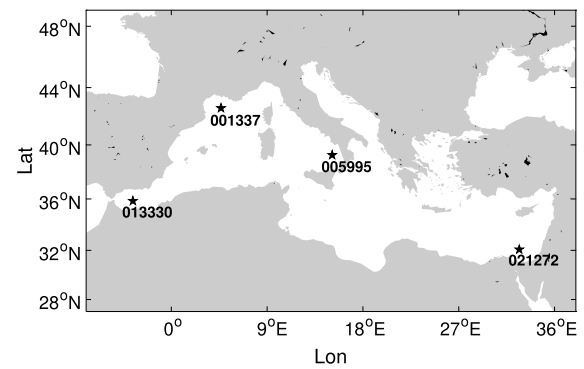


Fig. 4. Locations of the hindcast points employed for the graphical comparison between b and δ_i .

Table 1

Values of ρ_s for the correlation between the series of sums of δ_i and b for the annual H_s statistics analysed.

| | $\sum \delta_{i,AM} - b_{AM}$ | $\sum \delta_{i,98} - b_{98}$ | $\sum \delta_{i,MEAN} - b_{MEAN}$ |
|----------|-------------------------------|-------------------------------|-----------------------------------|
| ρ_s | 0.79 | 0.67 | 0.85 |

Table 2

Number of location characterized by trends at the 5% level and, in brackets, percentage referred to the total number of hindcast points (22373, see Mentaschi et al., 2013, 2015).

| AM | Annual 98th percentile | Annual mean |
|-------------|------------------------|--------------|
| 276 (1.23%) | 545 (2.44%) | 146 (0.65%) |
| 763 (3.41%) | 20 (0.09%) | 1078 (4.82%) |

cases, only the results of the ρ_s series are shown (Fig. 3 panel (b) and panel (c)).

As explained in Section 2.3.2, the series of b were further compared to the ITA results. To this end, four AM H_s series were analysed; they are characterized by either very intense trends (Point_001337 and Point_005995, upward and downward trend respectively), and by almost flat trends (Point_013330 and Point_021272), according to the values of the respective b_{AM} . Then, the ecdf of the respective δ_i were computed.

The locations of the hindcast points taken into account are shown in Fig. 4, while the AM H_s series of the selected locations are shown in Fig. 5. As Fig. 6 shows, the series with almost flat trends (e.g. b close to zero, panels (c)-(d) of Fig. 5) show δ_i with an approximately vertical profile in the ecdf space; on the other hand, series related to steeper trends (panels (a)-(b) of Fig. 5) are characterized by δ_i more shifted from the 0 line (which indicates the no-trend condition). This analysis reveals how the slope of the linear trend b is proportional to the magnitude of δ_i , i.e. the trend intensity according to the ITA approach. This applies to both upward (positive slopes, panel (a) of Fig. 6) and downward (negative slopes, panel (b) of Fig. 6) trends.

At a second time, ρ_s was computed using the sum of δ_i and b for all the populations considered (the subscripts AM, 98 and MEAN are used for δ_i and for b). Results are shown in Table 1, from which it appears that b_{AM} and b_{MEAN} have similar ρ_s , while the correlation is slightly lower between b_{98} and the respective δ_i .

3.2. Wave climate trends in the Mediterranean sea

First, it is interesting to analyse the spatial distribution of H_s trends when the most common usage of the MK, relying on the threshold $\alpha = 0.05$, is applied. Fig. 7 shows only the locations characterized by trends according to the aforementioned method for the AM data, annual 98th percentile, and annual mean H_s (panels (a), (b) and (c) of Fig. 7). The sign of the trends is computed using Eq. (7). The AM H_s results show

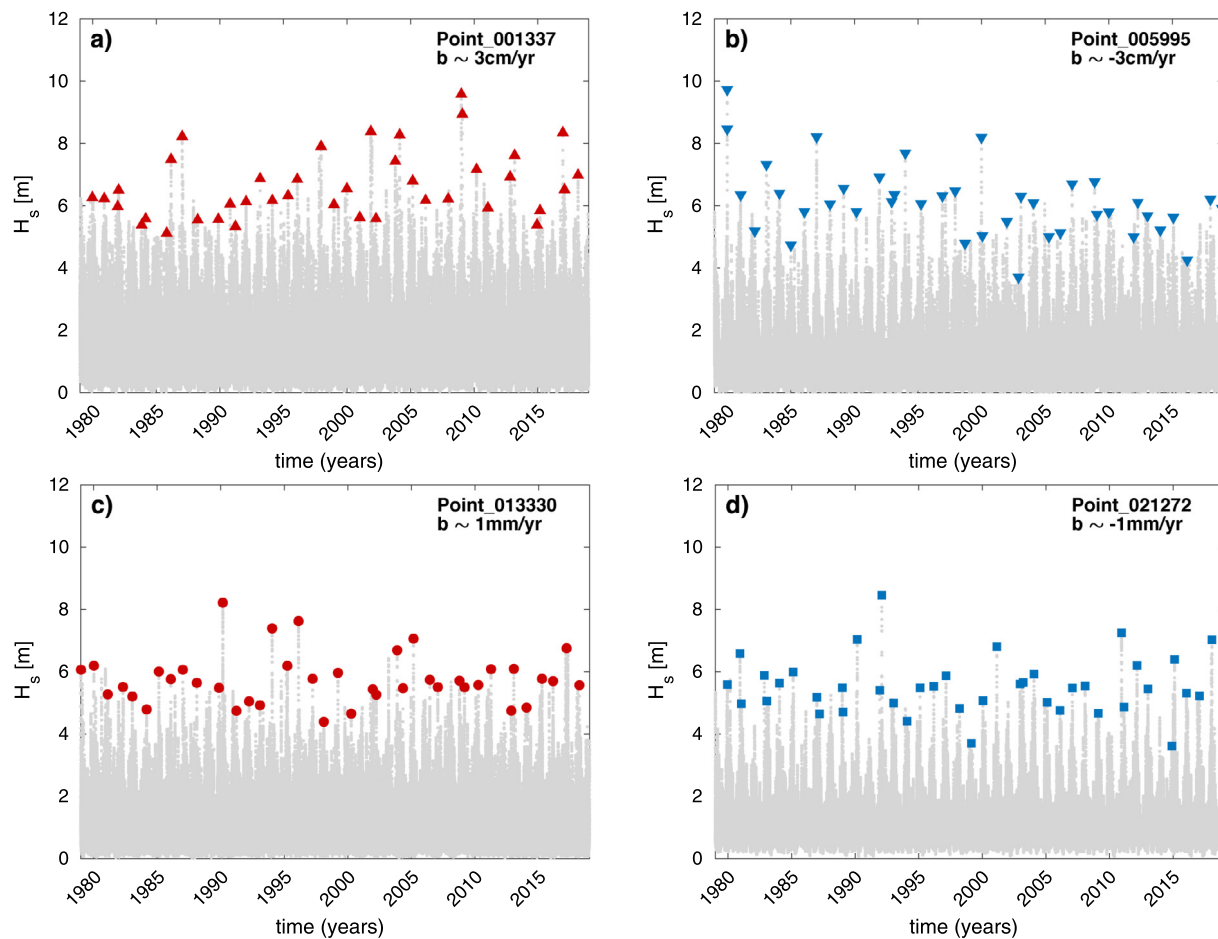


Fig. 5. Panels (a) and (c): AM H_s series with respective TS slopes for upward trends. Panels (b) and (d): downward trends. Red markers: AM H_s characterized by positive trends; blue markers: AM H_s characterized by negative trends; grey markers: original time series. (For interpretation of the references to colour in this figure legend, the reader is referred to the web version of this article.)

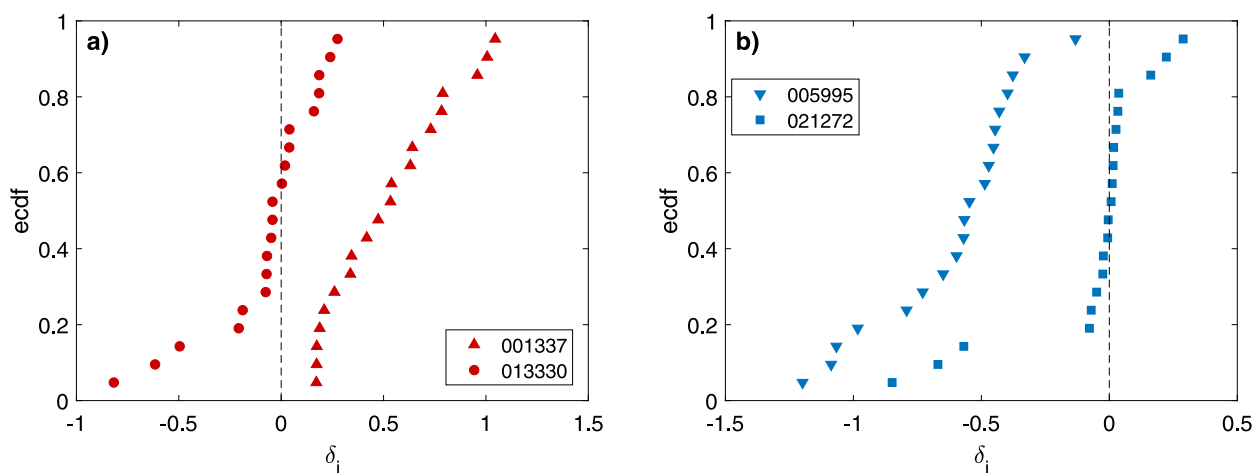


Fig. 6. δ_i ecdf for the locations characterized by different trend intensities for AM H_s series shown in Fig. 5. Panel (a): positive trends; panel (b): negative trends.

large areas characterized by negative trends in the south Tyrrhenian Sea and in the Ionian Sea, while smaller areas and isolated spots showing positive trends are present, for instance, in south-east of the Aegean Sea and in the northernmost areas of the MS. The results for the annual 98th percentile of H_s show positive trends in the south of the MS between Sicily and Libya, while negative trends are limited to very few locations. Results for the annual mean H_s show negative trends limited to the south-east basin of the MS and positive trends limited

to small spots in front of the Libyan coast and along the coastlines of Italy and Greece. The number of locations (grid points) characterized by trends for each annual statistic and $\alpha = 0.05$ is reported in Table 2.

On the other hand, Fig. 8 shows the values of b computed for the annual statistics of H_s over the MS, for both downward and upward trends. It can be seen that the most significant b for the AM H_s are between -5 cm/year and 3 cm/year. The areas subjected to the most intense negative trends are the south of the Tyrrhenian Sea (in front of

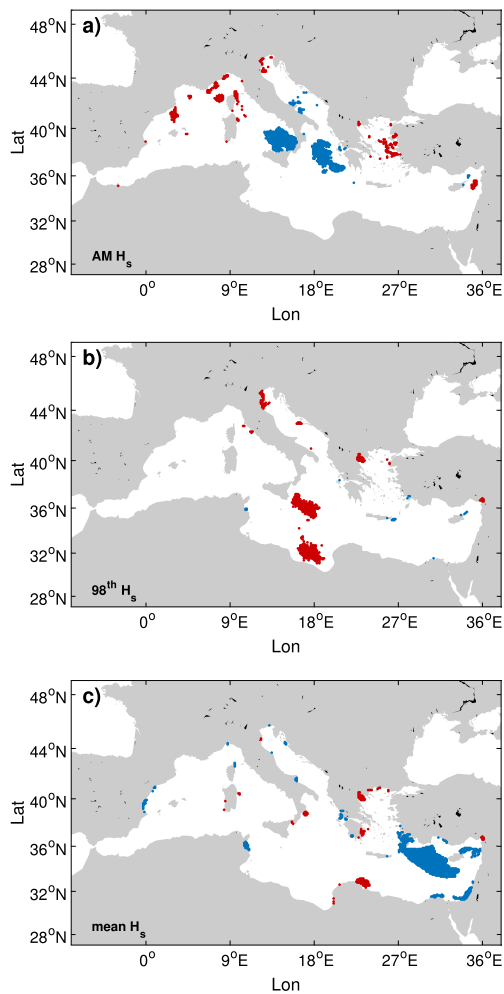


Fig. 7. Locations characterized by MK trends for α equal 0.05. Panel (a): AM H_s ; panel (b): annual 98th percentile of H_s ; panel (c): annual mean H_s . Red dots indicate positive trends, blue dots indicate negative trends. (For interpretation of the references to colour in this figure legend, the reader is referred to the web version of this article.)

the northern coasts of Calabria and Sicily) and the Ionian Sea, opposite the Greek coasts. On the other hand, the Aegean Sea and the Tyrrhenian Sea (on east Corsica and Sardinia), together with areas spread within the Balearic Sea, show wide areas subject to positive trends of the AM H_s . Results for the mean and the 98th percentile of H_s change dramatically with respect to those of AM H_s , especially for the trend intensities; indeed, in this case the trends show magnitude of mm/year. Both b_{MEAN} and b_{98} show areas with negative trends in the south-east of the MS and in the north Tyrrhenian Sea, while positive trends are found especially in the west of Sardinia and in the area between Libya and the Ionian Sea.

To the best of our knowledge, it is the first time that an analysis of wave climate trends is performed on the whole MS with such a resolution. Therefore, comparison to previous results can be carried out only considering of local trends analysis in the literature. Casas-Prat and Sierra Pedrico (2010a) and Casas-Prat and Sierra Pedrico (2010b) evaluated trends for different directional sectors along the Catalan coast; Piscopia et al. (2003) carried out a study on the Italian seas. However, in the aforementioned works trends were computed considering sea storms extracted by de-clustering threshold exceedance within the POT approach, thus a direct comparison with the present analysis would be not significant. Pomaro et al. (2017) evaluated trends on several monthly percentiles of H_s in the northern Adriatic Sea, showing a reduction in extremes and an increase in storminess that

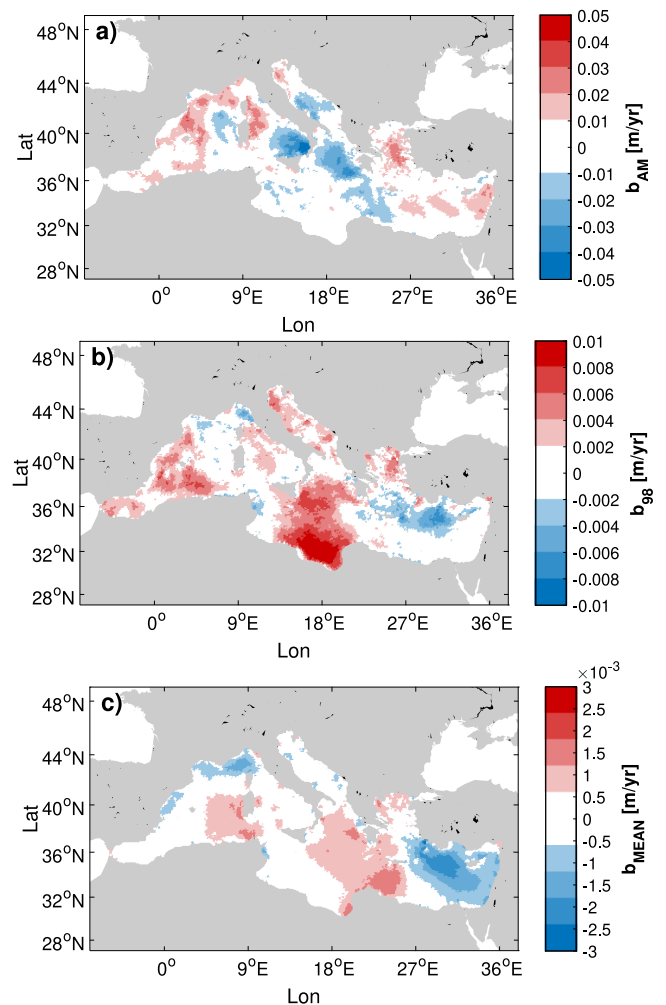


Fig. 8. Spatial distribution of b in the MS. From top to bottom: Panel (a): b_{AM} ; panel (b): b_{98} ; panel (c): b_{MEAN} .

is not fully consistent with the results of Fig. 8, where b_{98} is positive but no trend in AM H_s is found. Statistics based on annual intervals in eastern Mediterranean were carried out by Musić and Nicković (2008), further employing a simple linear regression for computing trends; their analysis of annual mean H_s returned negative trends of order of magnitude consistent with the present work, however, in their research, no positive trend is identified. As for their AM H_s analysis, local analysis within the Aegean Sea agrees qualitatively well with the outcomes of the present work. On the other hand, Musić and Nicković (2008) showed a slightly negative trend in front of the coast of Lebanon, while the present analysis suggests an area subject to homogeneous positive trends. On the contrary, the trend for 90th percentile in the same area is positive and apparently more consistent with the outcomes of the present work for the annual 98th percentile of H_s .

4. Discussion and conclusions

In most of the studies that use the MK, p_{MK} is evaluated against a threshold value of α to check for the presence of a trend. In the present work, by using the Spearman index as measure of correlation it was found that for the typical values of α used, the values of b do not appear to be strongly related to the p_{MK} they refer to. Therefore, in this case no useful considerations can be inferred for b , regardless the assumptions made about the use of p_{MK} . When p_{MK} is considered in its whole range, a clear anti-correlation with b can be instead appreciated.

In this case, it follows that the magnitude of b can be reasonably retained to evaluate how strong is the increasing/decreasing trend of the dataset under study. Indeed, the MK null hypothesis is the absence of a trend in a dataset. Close-to -0 values of p_{MK} mean that the data behave consistently with the presence of a marked trend (i.e. the null hypothesis is rejected), and this is more likely to occur for high values of b , as shown in Fig. 2 for the AM H_s (similar considerations hold for annual 98th percentile of H_s and annual mean H_s). On the contrary, close-to -1 values of p_{MK} are in turn related to low values of b ; in this case, trends on the data seem not to be relevant. When very mild values of b are observed (i.e. order of mm/year), a further check on the significance of such parameter could be suggested, as an instance computing its confidence interval (Wilcox, 2010) and evaluating if the limits indicate trends of different signs. A similar approach was used by Vanem (2015), who evaluated the reliability of non-stationary EVA on the basis of the location parameter fitted to the non-stationary GEV. At a second time, b was shown to be correlated with the ITA outcomes. In fact, both the graphical analysis of the δ_i ecdf for the selected locations, and the correlation analysis of the sum of δ_i for all the hindcast locations, reveal a strong correlation of δ_i itself and b , in particular for the annual mean and maxima H_s (as shown in Table 1). It follows that, in this case, the use of b for the quantification of trends is sound and reliable, because of the correlation with two methods that do not rely on the linear trend hypothesis. In the case of the MK, the application here considered takes advantage of the general use of p_{MK} , as recommended in Greenland et al. (2016), and allows to attach to each value of b a measure of the consistency with the null hypothesis, without any *a priori* selection based on a threshold level.

In view of the above, the values of b were used to gain an insight into the spatial distribution of wave climate trends over the MS. In particular, the statistics employed in this work were selected as they can be of great importance in maritime and ocean engineering. The AM H_s are indicative of the most severe sea states, which are retained to compute the high return period distribution of H_s , to be further used in marine and coastal structural design. In the framework of Extreme Value Analysis, the 98th percentile of the initial H_s distribution of a sample is often used as a threshold to select the exceeding peaks in the POT approach. Finally, mean sea states can be relevant for fatigue analysis of maritime structures. The analysis revealed similar patterns among the spatial distributions of trends for the annual 98th percentile of H_s and annual mean H_s , with variations in order of mm/year. Nevertheless, it should be pointed out that such trends are not much relevant from a practical point of view, e.g. the design of maritime structures would not be significantly affected by H_s variations of centimetres in time frames of decades. Moreover, uncertainties may arise due to the resolution of the numerical model used to build the hindcast. On the other hand, trends of AM H_s are characterized by more intense values of b (order of cm/year). In the latter case, some analogies can be appreciated with the spatial distribution of trends in the 98th percentile of H_s , in particular in the North Adriatic Sea, in the Aegean Sea and in the Balearic area. On the contrary, the main divergences interest the Southern part of the Ionian and Adriatic Seas, the Levantine basin and in the Tyrrhenian Sea. These differences can be explained considering how the different dataset are selected: annual percentiles average on huge amount of data, therefore are lowered by mild sea states that, being more frequent, matter the most. This reflects on the distribution of the dataset considered for the wave heights trend evaluation, which in case of the AM H_s happen to be more dispersed.

These outcomes were then compared to previous researches aimed at detecting and computing trends over isolated spots in the MS. The order of magnitude of the annual rate of changes show good consistency with the values of b computed in this work, while there are slight deviations in the sign of trends for some locations, as discussed in Section 3.2. However, it has to be reminded that the exhaustively characterization of the wave climate trends in the MS is beyond the scope of this research, though interesting analogies with previous works

can be pointed out and leave room for further investigation. In particular, the results in this study show some analogy with the results presented in Young and Ribal (2019). In both cases there is evidence that trends in H_s are stronger for high percentiles compared to annual averages; Young and Ribal (2019) explains this with trends in the wind speed distribution, that are matched by the trends in the distribution of H_s globally. Also, regional variations are significant in the present study and stronger trends appear in more energetic parts of the basin (e.g. in the West Mediterranean). Finally, it is worth mentioning that, although the paper focuses on sea waves, the analysis here introduced can be extended to other parameters without loss of generality, and its application to different geophysical time series is therefore straightforward.

Declaration of competing interest

The authors declare that they have no known competing financial interests or personal relationships that could have appeared to influence the work reported in this paper.

CRedit authorship contribution statement

Francesco De Leo: Conceptualization, Data curation, Formal analysis, Software, Investigation, Methodology, Writing - original draft, Writing - review & editing. **Annalisa De Leo:** Investigation, Methodology, Data curation, Writing - review & editing. **Giovanni Besio:** Conceptualization, Data curation, Supervision, Writing - review & editing. **Riccardo Briganti:** Conceptualization, Investigation, Methodology, Supervision, Writing - review & editing.

Acknowledgements

The results for b and p_{MK} are available for download at Nottingham Research Data Management Repository, doi: <http://dx.doi.org/10.17639/nott.7016>

References

- Adger, W.N., 1999. Social vulnerability to climate change and extremes in coastal Vietnam. *World Dev.* 27, 249–269.
- Appendini, C.M., Torres-Freyermuth, A., Salles, P., López-González, J., Mendoza, E.T., 2014. Wave climate and trends for the Gulf of Mexico: A 30-yr wave hindcast. *J. Clim.* 27, 1619–1632.
- Besio, G., Briganti, R., Romano, A., Mentaschi, L., De Girolamo, P., 2017. Time clustering of wave storms in the Mediterranean Sea. *Nat. Hazards Earth Syst. Sci.* 17, 505–514.
- Bonett, D.G., Wright, T.A., 2000. Sample size requirements for estimating Pearson, Kendall and Spearman correlations. *Psychometrika* 65, 23–28.
- Burke, E.J., Perry, R.H., Brown, S.J., 2010. An extreme value analysis of UK drought and projections of change in the future. *J. Hydrol.* 388, 131–143.
- Cai, W., Cowan, T., 2007. Trends in Southern Hemisphere circulation in IPCC AR4 models over 1950–99: Ozone depletion versus greenhouse forcing. *J. Clim.* 20, 681–693.
- Cai, W., Shi, G., Cowan, T., Bi, D., Ribbe, J., 2005. The response of the Southern Annular Mode, the East Australian Current, and the southern mid-latitude ocean circulation to global warming. *Geophys. Res. Lett.* 32.
- Casas-Prat, M., Sierra Pedrico, J.P., 2010a. Trend analysis of the wave storminess: the wave direction. *Adv. Geosci.* 26, 89–92.
- Casas Prat, M., Sierra Pedrico, J.P., 2010b. Trend analysis of wave storminess: wave direction and its impact on harbour agitation. *Nat. Hazards Earth Syst. Sci.* 10, 2327–2340.
- Castelle, B., Dodet, G., Masselink, G., Scott, T., 2018. Increased winter-mean wave height, variability, and periodicity in the Northeast Atlantic over 1949–2017. *Geophys. Res. Lett.* 45, 3586–3596.
- Coles, S., Bawa, J., Trenner, L., Dorazio, P., 2001. *An Introduction to Statistical Modeling of Extreme Values*. Vol. 208. Springer.
- Şen, Z., 2011. Innovative trend analysis methodology. *J. Hydrol. Eng.* 17, 1042–1046.
- Şen, Z., 2013. Trend identification simulation and application. *J. Hydrol. Eng.* 19, 635–642.
- De Leo, F., Besio, G., Zolezzi, G., Bezzi, M., 2019. Coastal vulnerability assessment: through regional to local downscaling of wave characteristics along the Bay of Lalzit (Albania). *Nat. Hazards Earth Syst. Sci.* 19, 287–298.

- De Michele, C., Salvadori, G., Passoni, G., Vezzoli, R., 2007. A multivariate model of sea storms using copulas. *Coast. Eng.* 54, 734–751.
- Dolan, A.H., Walker, I.J., 2006. Understanding vulnerability of coastal communities to climate change related risks. *J. Coast. Res.* 131, 6–1323.
- Doney, S.C., Ruckelshaus, M., Emmett Duffy, J., Barry, J.P., Chan, F., English, C.A., Galindo, H.M., Grebmeier, J.M., Hollowed, A.B., Knowlton, N., et al., 2012. Climate change impacts on marine ecosystems. *Ann. Rev. Mar. Sci.* 4, 11–37.
- Durack, P.J., Wijffels, S.E., 2010. Fifty-year trends in global ocean salinities and their relationship to broad-scale warming. *J. Clim.* 23, 4342–4362.
- Genest, C., Favre, A.C., 2007. Everything you always wanted to know about copula modeling but were afraid to ask. *J. Hydrol. Eng.* 12, 347–368.
- Greenland, S., Senn, S.J., Rothman, K.J., Carlin, J.B., Poole, C., Goodman, S.N., Altman, D.G., 2016. Statistical tests, P values, confidence intervals, and power: a guide to misinterpretations. *Eur. J. Epidemiol.* 31, 337–350.
- Gulev, S.K., Grigorieva, V., 2004. Last century changes in ocean wind wave height from global visual wave data. *Geophys. Res. Lett.* 31.
- Hamm, L., Capobianco, M., Dette, H., Lechuga, A., Spanhoff, R., Stive, M., 2002. A summary of European experience with shore nourishment. *Coast. Eng.* 47, 237–264.
- Harley, C.D., Randall Hughes, A., Hultgren, K.M., Miner, B.G., Sorte, C.J., Thornber, C.S., Rodriguez, L.F., Tomanek, L., Williams, S.L., 2006. The impacts of climate change in coastal marine systems. *Ecol. Lett.* 9, 228–241.
- Kendall, M.G., 1955. Rank correlation methods.
- Koetse, M.J., Rietveld, P., 2009. The impact of climate change and weather on transport: An overview of empirical findings. *Transp. Res. D* 14, 205–221.
- Laface, V., Malara, G., Romolo, A., Arena, F., 2016. Peak over threshold vis-à-vis equivalent triangular storm: Return value sensitivity to storm threshold. *Coast. Eng.* 116, 220–235.
- Liang, B., Shao, Z., Li, H., Shao, M., Lee, D., 2019. An automated threshold selection method based on the characteristic of extrapolated significant wave heights. *Coast. Eng.* 144, 22–32.
- Mann, H.B., 1945. Nonparametric tests against trend. *Econometrica: J. Econom. Soc.* 24, 5–259.
- Méndez, F.J., Menéndez, M., Luceño, A., Losada, I.J., 2006. Estimation of the long-term variability of extreme significant wave height using a time-dependent Peak Over Threshold (POT) model. *J. Geophys. Res.: Oceans* 111.
- Mentaschi, L., Besio, G., Cassola, F., Mazzino, A., 2013. Developing and validating a forecast/hindcast system for the Mediterranean Sea. *J. Coast. Res.* SI 65, 1551–1556.
- Mentaschi, L., Besio, G., Cassola, F., Mazzino, A., 2015. Performance evaluation of WavewatchIII in the Mediterranean Sea. *Ocean Model.* 90, 82–94.
- Mentaschi, L., Voudoukas, M., Voukouvalas, E., Sartini, L., Feyen, L., Besio, G., Alfieri, L., 2016. Non-stationary extreme value analysis: a simplified approach for earth science applications. *Hydrol. Earth Syst. Sci. Discuss.* 2016, 1–38.
- Mori, N., Yasuda, T., Mase, H., Tom, T., Oku, Y., 2010. Projection of extreme wave climate change under global warming. *Hydrol. Res. Lett.* 4, 15–19.
- Morim, J., Hemer, M., Wang, X.L., Cartwright, N., Trenham, C., Semedo, A., Young, I., Bricheno, L., Camus, P., Casas-Prat, M., et al., 2019. Robustness and uncertainties in global multivariate wind-wave climate projections. *Nature Clim. Change* 9, 711–718.
- Muraleedharan, G., Lucas, C., Soares, C.G., 2016. Regression quantile models for estimating trends in extreme significant wave heights. *Ocean Eng.* 118, 204–215.
- Musić, S., Nicković, S., 2008. 44-year wave hindcast for the Eastern Mediterranean. *Coast. Eng.* 55, 872–880.
- Nicholls, R.J., Cazenave, A., 2010. Sea-level rise and its impact on coastal zones. *Science* 328, 1517–1520.
- Piscopia, R., Inghilesi, R., Panizzo, A., Corsini, S., Franco, L., 2003. Analysis of 12-year wave measurements by the Italian Wave Network. In: *Coastal Engineering 2002: Solving Coastal Conundrums*. World Scientific, pp. 121–133.
- Pomaro, A., Cavaleri, L., Lionello, P., 2017. Climatology and trends of the Adriatic Sea wind waves: analysis of a 37-year long instrumental data set. *Int. J. Climatol.* 37, 4237–4250.
- Richards, J., Mokrech, M., Berry, P., Nicholls, R., 2008. Regional assessment of climate change impacts on coastal and fluvial ecosystems and the scope for adaptation. *Clim. Change* 90, 141–167.
- Saha, S., Moorthi, S., Pan, H.L., Wu, X., Wang, J., Nadiga, S., Tripp, P., Kistler, R., Woollen, J., Behringer, D., Liu, H., Stokes, D., Grubine, R., Gayno, G., Wang, J., Hou, Y.T., Chuang, H.Y., Juang, H.M.H., Sela, J., Iredell, M., Treadon, R., Kleist, D., Van Delst, P., Keyser, D., Derber, J., Ek, M., Meng, J., Wei, H., Yang, R., Lord, S., Van Den Dool, H., Kumar, A., Wang, W., Long, C., Chelliah, M., Xue, Y., Huang, B., Schemm, J.K., Ebisuzaki, W., Lin, R., Xie, P., Chen, M., Zhou, S., Higgins, W., Zou, C.Z., Liu, Q., Chen, Y., Han, Y., Cucurull, L., Reynolds, R.W., Rutledge, G., Goldberg, M., 2010. The NCEP climate forecast system reanalysis. *Bull. Amer. Meteorol. Soc.* 91, 1015–1057.
- Scavia, D., Field, J.C., Boesch, D.F., Buddemeier, R.W., Burkett, V., Cayan, D.R., Fogarty, M., Harwell, M.A., Howarth, R.W., Mason, C., et al., 2002. Climate change impacts on US coastal and marine ecosystems. *Estuaries* 25, 149–164.
- Sen, P.K., 1968. Estimates of the regression coefficient based on Kendall's tau. *J. Amer. Statist. Assoc.* 63, 1379–1389.
- Shanas, P., Kumar, V.S., 2015. Trends in surface wind speed and significant wave height as revealed by ERA-Interim wind wave hindcast in the Central Bay of Bengal. *Int. J. Climatol.* 35, 2654–2663.
- Shi, J., Zheng, J., Zhang, C., Joly, A., Zhang, W., Xu, P., Sui, T., Chen, T., 2019. A 39-year high resolution wave hindcast for the Chinese coast: Model validation and wave climate analysis. *Ocean Eng.* 183, 224–235.
- Skamarock, W., Klemp, J., Dudhia, J., Gill, D., Barker, D., Wang, W., Powers, J., 2008. A Description of the Advanced Research WRF Version 3. Technical Note TN-468+STR, NCAR, p. 113.
- Solari, S., Egüen, M., Polo, M.J., Losada, M.A., 2017. Peaks over threshold (POT): A methodology for automatic threshold estimation using goodness of fit p-value. *Water Resour. Res.* 53, 2833–2849.
- Stive, M.J., 2004. How important is global warming for coastal erosion? *Clim. Change* 64, 27–39.
- Theil, H., 1992. A rank-invariant method of linear and polynomial regression analysis. In: *Henri Theil's Contributions To Economics and Econometrics*. Springer, pp. 345–381.
- Tolman, H.L., 2009. User Manual and System Documentation of WAVEWATCH III Version 3.14. Technical Report. NOAA/NWS/NCEP/MMAB.
- Vanem, E., 2015. Non-stationary extreme value models to account for trends and shifts in the extreme wave climate due to climate change. *Appl. Ocean Res.* 52, 201–211.
- Vanem, E., 2016. Joint statistical models for significant wave height and wave period in a changing climate. *Mar. Struct.* 49, 180–205.
- Vanem, E., Walker, S.E., 2013. Identifying trends in the ocean wave climate by time series analyses of significant wave height data. *Ocean Eng.* 61, 148–160.
- Wang, X.L., Trewin, B., Feng, Y., Jones, D., 2013. Historical changes in Australian temperature extremes as inferred from extreme value distribution analysis. *Geophys. Res. Lett.* 40, 573–578.
- Wasserstein, R.L., Lazar, N.A., et al., 2016. The ASA's statement on p-values: context, process, and purpose. *Amer. Statist.* 70, 129–133.
- Wdowinski, S., Bray, R., Kirtman, B.P., Wu, Z., 2016. Increasing flooding hazard in coastal communities due to rising sea level: Case study of Miami Beach, Florida. *Ocean Coast. Manage.* 126, 1–8.
- Weisse, R., 2010. *Marine Climate and Climate Change: Storms, Wind Waves and Storm Surges*. Springer Science & Business Media.
- Wilcox, R.R., 2010. *Fundamentals of Modern Statistical Methods: Substantially Improving Power and Accuracy*. Springer.
- Young, I.R., Ribal, A., 2019. Multiplatform evaluation of global trends in wind speed and wave height. *Science* 364, 548–552.
- Zar, J.H., 2005. Spearman rank correlation. *Encyclopedia Biostat.* 7.